


Doxorubicin-induced cardiovascular toxicity: a longitudinal evaluation of functional and molecular markers

Matthias Bosman ^{1*}, Dustin Krüger¹, Charles Van Assche², Hanne Boen^{3,4}, Cédric Neutel¹, Kasper Favere^{1,3,4}, Constantijn Franssen^{3,4}, Wim Martinet¹, Lynn Roth¹, Guido R. Y. De Meyer¹, Berta Cillero-Pastor^{2,5}, Leen Delrue⁶, Ward Heggermont^{6,7}, Emeline M. Van Craenenbroeck^{3,4}, and Pieter-Jan Guns¹

¹Laboratory of Physiopharmacology, Faculty of Medicine and Health Sciences, Faculty of Pharmaceutical, Biomedical and Veterinary Sciences, Campus Drie Eiken, University of Antwerp, Universiteitsplein 1, Antwerp B-2610, Belgium; ²Research Group M4I—Imaging Mass Spectrometry (IMS); Faculty of Health, Medicine and Life Sciences, Maastricht MultiModal Molecular Imaging Institute, Maastricht University, Universiteitssingel 50, 6229 ER, Maastricht, The Netherlands; ³Research Group Cardiovascular Diseases, GENCOR, University of Antwerp, Antwerp B-2610, Belgium; ⁴Department of Cardiology, Antwerp University Hospital (UZA), Drie Eikenstraat 655, Edegem B-2650, Belgium; ⁵Department of Cell Biology-Inspired Tissue Engineering, Institute for Technology-Inspired Regenerative Medicine, Universiteitssingel 40, 6229 ER Maastricht/Room C3.577, PO Box 616, Maastricht 6200 MD, The Netherlands; ⁶Department of Cardiology, Cardiovascular Center OLV Hospital Aalst, Moorselbaan 164, Aalst B-9300, Belgium; and ⁷Department of Cardiology, Center for Molecular and Vascular Biology, KU Leuven, Herestraat 49, Leuven B-3000, Belgium

Received 23 September 2022; revised 19 June 2023; accepted 27 July 2023; online publish-ahead-of-print 25 August 2023

Aims

Apart from cardiotoxicity, the chemotherapeutic doxorubicin (DOX) induces vascular toxicity, represented by arterial stiffness and endothelial dysfunction. Both parameters are of interest for cardiovascular risk stratification as they are independent predictors of future cardiovascular events in the general population. However, the time course of DOX-induced cardiovascular toxicity remains unclear. Moreover, current biomarkers for cardiovascular toxicity prove insufficient. Here, we longitudinally evaluated functional and molecular markers of DOX-induced cardiovascular toxicity in a murine model. Molecular markers were further validated in patient plasma.

Methods and results

DOX (4 mg/kg) or saline (vehicle) was administered intra-peritoneally to young, male mice weekly for 6 weeks. *In vivo* cardiovascular function and *ex vivo* arterial stiffness and vascular reactivity were evaluated at baseline, during DOX therapy (Weeks 2 and 4) and after therapy cessation (Weeks 6, 9, and 15). Left ventricular ejection fraction (LVEF) declined from Week 4 in the DOX group. DOX increased arterial stiffness *in vivo* and *ex vivo* at Week 2, which reverted thereafter. Importantly, DOX-induced arterial stiffness preceded reduced LVEF. Further, DOX impaired endothelium-dependent vasodilation at Weeks 2 and 6, which recovered at Weeks 9 and 15. Conversely, contraction with phenylephrine was consistently higher in the DOX-treated group. Furthermore, proteomic analysis on aortic tissue identified increased thrombospondin-1 (THBS1) and alpha-1-antichymotrypsin (SERPINA3) at Weeks 2 and 6. Up-regulated THBS1 and SERPINA3 persisted during follow-up. Finally, THBS1 and SERPINA3 were quantified in plasma of patients. Cancer survivors with anthracycline-induced cardiotoxicity (AICT; LVEF < 50%) showed elevated THBS1 and SERPINA3 levels compared with age-matched control patients (LVEF ≥ 60%).

Conclusions

DOX increased arterial stiffness and impaired endothelial function, which both preceded reduced LVEF. Vascular dysfunction restored after DOX therapy cessation, whereas cardiac dysfunction persisted. Further, we identified SERPINA3 and THBS1 as promising biomarkers of DOX-induced cardiovascular toxicity, which were confirmed in AICT patients.

Translational perspective

DOX induced arterial stiffness and endothelial dysfunction, which preceded impairment of left ventricular systolic function. Hence, arterial stiffness and endothelial dysfunction represent potential early, functional markers of future cardiovascular dysfunction in patients receiving DOX. Of note, DOX-induced arterial stiffness and endothelial dysfunction were transient, highlighting the importance of timing for evaluating these vascular parameters in patients. Furthermore, anthracycline-induced cardiotoxicity patients showed elevated SERPINA3 and THBS1 in plasma, raising awareness for a role of these proteins in cardiovascular toxicity with possible diagnostic value in DOX-treated patients.

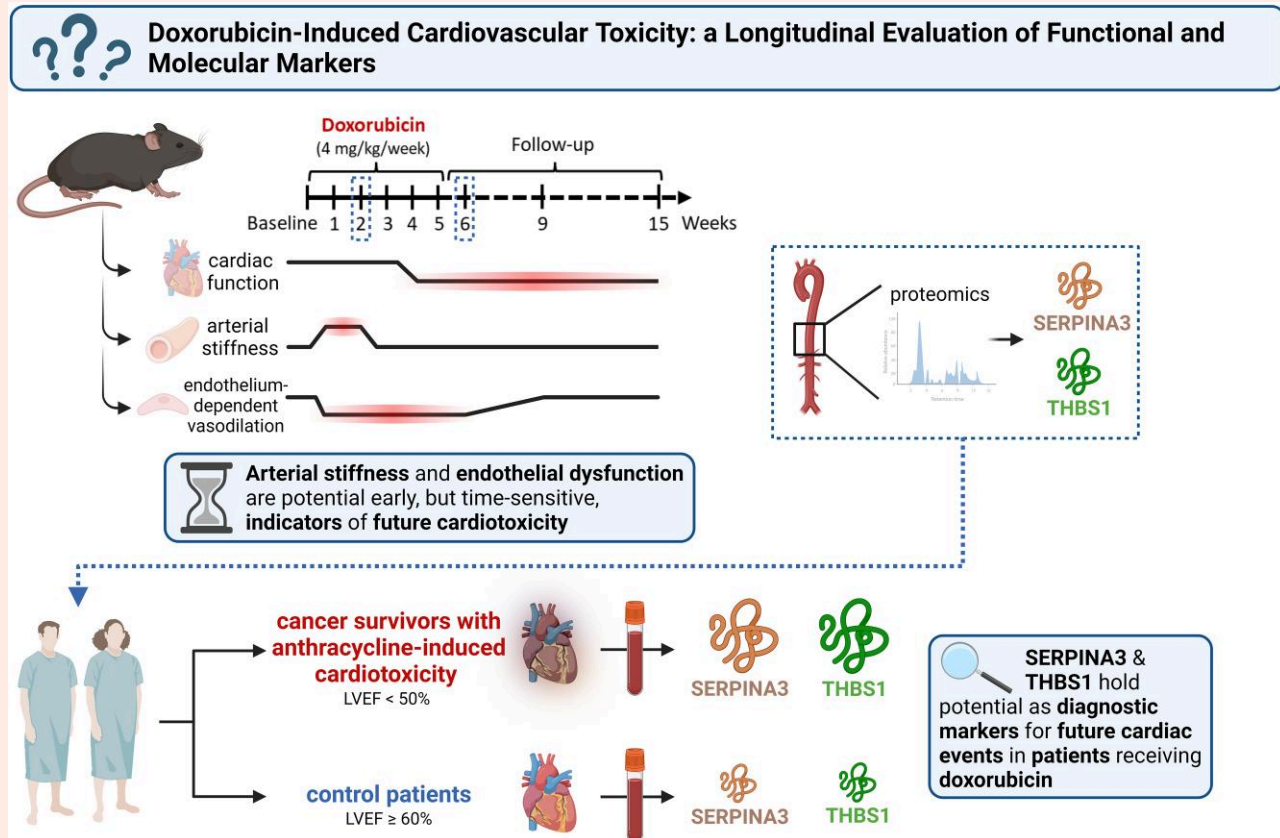
* Corresponding author. Tel: +32 (0) 3 265 2784, E-mail: matthias.bosman@uantwerpen.be

The Laboratory of Physiopharmacology and the Research Group Cardiovascular Diseases are part of the Infra-Med Centre of Excellence of the University of Antwerp.

© The Author(s) 2023. Published by Oxford University Press on behalf of the European Society of Cardiology.

This is an Open Access article distributed under the terms of the Creative Commons Attribution-NonCommercial License (<https://creativecommons.org/licenses/by-nc/4.0/>), which permits non-commercial re-use, distribution, and reproduction in any medium, provided the original work is properly cited. For commercial re-use, please contact journals.permissions@oup.com

Graphic Abstract



Keywords

Doxorubicin • Arterial stiffness • Endothelial dysfunction • Cardiotoxicity

1. Introduction

Doxorubicin (DOX), an anthracycline, is a potent chemotherapeutic agent in the treatment of breast cancer, leukaemia, and lymphoma.¹ Today, it has been estimated that more than half of lymphoma and childhood cancers and one-third of breast cancers are treated with a DOX-based regimen.² However, DOX can cause cardiotoxicity and eventually lead to heart failure (HF),^{3,4} which has been extensively investigated in the past (reviewed elsewhere⁵). Interestingly, concomitant presence of modifiable risk factors, such as systemic hypertension, further potentiates the likelihood for cardiovascular events in DOX-treated cancer survivors.⁶ Therefore, DOX-induced vascular toxicity could be an early indicator of future cardiovascular events.

Among representations of vascular toxicity, enhanced arterial stiffness and endothelial dysfunction are of particular interest for cardiovascular risk assessment as they have previously been shown to independently predict future cardiovascular events in the general population.^{7–12} Despite clinical trials reporting increased arterial stiffness and impaired cardiac function after 3–6 months of DOX therapy initiation,^{13–17} the temporal relationship between these events has not been characterized. Moreover, it remains unclear whether arterial stiffness is reversible after DOX therapy cessation. Finally, while some childhood cancer survivors exhibit endothelial dysfunction months to years after anthracycline therapy completion,^{18,19} development of endothelial dysfunction has not been longitudinally investigated so far.

Furthermore, current biomarkers for identification of early myocardial damage in DOX-treated patients prove insufficient. While circulating troponin and (N-terminal pro-)B-type natriuretic peptide show promise to identify patients at cardiac risk, these proteins do not predict adverse cardiac outcome in every subject.^{20,21} A broadening of the biomarker panel is therefore recommended by the current European Society of Cardiology (ESC) guidelines on cardio-oncology.²²

Here, in a murine model, we evaluated cardiovascular function both during and after DOX therapy to characterize the time course of DOX-induced cardiovascular toxicity. In addition, a proteomic approach was implemented to identify new potential biomarkers, which were further clinically validated.

2. Materials and methods

2.1 Animals and ethical approval

Male C57BL/6J mice (Charles River, France) with an age between 10 and 12 weeks and a body weight between 26 and 30 g were used in all experiments. All mice were housed in the animal facility of the University of Antwerp in standard cages with 12- to 12-h light/dark cycles with access to regular chow and water *ad libitum*. The Ethical Committee of the University of Antwerp approved all experiments (file 2019-34 and 2020-74), which were conform to Directive 2010/63/EU, the ARRIVE guidelines, and the Guide for the Care and Use of Laboratory Animals

published by the US National Institutes of Health (NIH Publication no. 85–23, revised 1996).

2.2 DOX treatment and experimental workflow

Mice were randomly divided into three cohorts of 16 mice each, namely, Cohort 1, Cohort 2, and Cohort 3. In each cohort, half of the mice were intra-peritoneally injected with either DOX (4 mg/kg; Adriamycin®, Pfizer, Puurs, Belgium) or vehicle (10 mL/kg of a 0.9% NaCl solution; B. Braun, Belgium) once per week for a total of 6 weeks. The first and final injections were administered at baseline (Week 0) and at Week 5, respectively. All cohorts received the same treatment regimen but differed in the duration of follow-up. There was 1 week of follow-up for Cohort 1 (up to Week 6), 4 weeks for Cohort 2 (up to Week 9), and 10 weeks for Cohort 3 (up to Week 15). For all cohorts, *in vivo* cardiovascular function was assessed at baseline, Week 2 and Week 6 with high-frequency ultrasound imaging. *In vivo* cardiovascular function was additionally evaluated at Week 4 for Cohort 1, at Week 9 for Cohort 2, and at Week 15 for Cohort 3. For *ex vivo* assessment of arterial stiffness and vascular reactivity and to perform molecular experiments, Cohorts 1, 2, and 3 were sacrificed at Weeks 6, 9, and 15, respectively. To this end, mice were euthanized by intraperitoneal injection of a single dose of sodium pentobarbital (200 mg/kg; Sanofi, Belgium), followed by perforation of the diaphragm (when under deep anaesthesia) in order to preserve vascular physiology and structure.

2.3 High-frequency ultrasound imaging

Ultrasound imaging was performed in anaesthetized mice under 1.5–2.5% (*v/v*) isoflurane (Forene; AbbVie, Wavre, Belgium) using a high-frequency ultrasound system (Vevo2100, VisualSonics, Toronto, Canada). Images were acquired with a 24 MHz transducer when heart rate and body temperature met the inclusion criteria, i.e. 500 ± 50 b.p.m. and $37 \pm 1^\circ\text{C}$, respectively. M-mode images were obtained for measurement of left ventricular anterior wall (LVAW) thickness, left ventricular posterior wall (LVPW) thickness, left ventricular internal diameter (LVID), and calculation of left ventricular ejection fraction (LVEF) and fractional shortening (FS) with Vevo LAB Software (Version 3.2.0, VisualSonics, Toronto, Canada). In the same session, abdominal aorta pulse wave velocity (aaPWV), a measure for *in vivo* arterial stiffness, was determined according to the method developed by Di Lascio *et al.*²³ Briefly, pulse wave Doppler tracing was used to measure aortic flow velocity (*V*). Immediately thereafter, aortic diameter (*D*) was measured on 700 frames-per-second B-mode images of the abdominal aorta in electrocardiogram-gated kilohertz visualization (EKV) imaging mode. The $\ln(D)$ -*V* loop method was then applied to calculate aaPWV, using MATLAB v2014 software (MathWorks, Eindhoven, the Netherlands).

2.4 Blood pressure evaluation

Systolic blood pressure (BP) and diastolic BP were determined non-invasively in restrained, awake mice using a tail-cuff system with a programmed electro-sphygmomanometer (Coda, Kent Scientific Corporation, Torrington, United States of America). Mice were trained for 2 days prior to the actual measurements to reduce stress and variability during measurements. To this end, the cuff system was placed on the mouse tail as performed during the actual measurements. The duration of the training and measurement sessions was 30 min. Measurements were only performed in Cohort 3 at baseline and at Weeks 2, 6, 9, and 15.

2.5 Ex vivo evaluation of aortic stiffness and vascular reactivity

Mice were intraperitoneally injected with sodium pentobarbital (single dose of 200 mg/kg; Sanofi, Belgium), followed by perforation of the diaphragm (under deep anaesthesia). The thoracic aorta was carefully dissected and cut into segments of 2 mm length, which were subsequently

mounted between two hooks of an organ bath set-up (10 mL) filled with Krebs-Ringer solution (37°C , 95% O_2 /5% CO_2 , pH 7.4) containing (in mmol/L) NaCl 118, KCl 4.7, CaCl_2 2.5, KH_2PO_4 1.2, MgSO_4 1.2, NaHCO_3 25, CaEDTA 0.025, and glucose 11.1.

Ex vivo assessment of aortic stiffness was performed with the in-house developed organ bath set-up, called 'Rodent Oscillatory Tension Set-up to Study Arterial Compliance' (ROTSAC) as previously described.^{24–26} In brief, segments were continuously stretched between alternating preloads corresponding to 'systolic' and 'diastolic' trans-mural pressures and at a physiological frequency of 10 Hz to mimic the physiological heart rate in mice (600 b.p.m.). Calibration of the set-up allows calculation of the Peterson's modulus (E_p), a measure of *ex vivo* arterial stiffness, based on LaPlace's equation. E_p was calculated as follows: $E_p = D_0 * \Delta P / \Delta D$, where ΔP is the difference in pressure (kept constant at 40 mmHg), D_0 is the 'diastolic' diameter, and ΔD is the change in diameter between 'diastolic' and 'systolic' pressure. The ROTSAC protocol included the evaluation of aortic stiffness (E_p) at 80–120 mmHg, under Krebs-Ringer, diethylamine NONOate (DEANO; 2 μM) and phenylephrine (PE; 2 μM) conditions. DEANO is an exogenous nitric oxide (NO) donor, which removes vascular tone and allows the investigation of the contribution of primarily passive/structural elements to aortic stiffness.²⁷ PE is an α_1 -adrenergic receptor agonist and allows the evaluation of vascular tone in aortic stiffness.

Ex vivo vascular reactivity was studied by mounting aortic segments at a preload of 20 mN. Since we have previously shown that basal NO declines over time,²⁸ the experimental protocol was started 70 min after puncture of the diaphragm to minimize time-dependent biases. Vascular smooth-muscle cell (VSMC) contraction was evaluated by adding cumulative concentrations of PE (3 nM to 10 μM). PE-induced contraction is repressed by basal NO.^{27,28} By performing PE-induced contraction after pre-incubation with the endothelial NO synthase (eNOS) inhibitor N^ω -nitro-L-arginine methyl ester (L-NAME; 300 μM) and comparing this with PE-induced contraction without L-NAME, the capability of endothelial cells (ECs) to produce basal NO can be investigated.^{27,28} Low basal NO levels lead to higher PE-induced contraction and similar contraction magnitude in the presence of L-NAME.^{27,28} Endothelium-dependent relaxation was investigated by addition of cumulative concentrations of acetylcholine (ACh) (3 nM to 10 μM), a muscarinic receptor agonist. Finally, endothelium-independent relaxation was evaluated by using different cumulative concentrations of DEANO (0.3 nM to 10 μM).

2.6 Western blotting

Aortic samples were lysed in Laemmli sample buffer (Bio-Rad, Temse, Belgium) containing 5% β -mercaptoethanol (Sigma-Aldrich, Overijse, Belgium) and subsequently heat-denatured for 5 min at 100°C . Next, samples were loaded on Bolt 4–12% Bis-Tris gels (Invitrogen, Merelbeke, Belgium) and after electrophoresis transferred to Immobilon-FL PVDF membranes (Merck, Hoeilaart, Belgium). Of note, no assay to determine the protein concentration could be performed prior to sample loading since only a limited amount of aortic sample was available (due to combination of vascular reactivity and arterial stiffness evaluation). After blocking (1 h, Odyssey Li-COR blocking buffer, Li-COR Biosciences, Bad Homburg, Germany), membranes were probed with primary antibodies, diluted in Odyssey Li-COR blocking buffer, overnight at 4°C . The following primary antibodies were used: rabbit anti-thrombospondin-1 (THBS1) (1:500; ab267388, Abcam, Cambridge, UK), goat anti-alpha-1-antichymotrypsin (SERPINA3) (1:1000; catalogue number AF4709, Bio-Techne, Dublin, Ireland) and mouse anti- β -actin (1:5000; ab8226, Abcam, Cambridge, UK). The next day, membranes were incubated with IRDye-labelled secondary antibodies (goat anti-rabbit IgG926–32211, donkey anti-goat IgG926–32214, and goat anti-mouse IgG926–68070, all purchased from Li-COR Biosciences, Bad Homburg, Germany) for 1 h at room temperature. Membranes were visualized with an Odyssey SA infrared imaging system (Li-COR Biosciences, Bad Homburg, Germany). Western blot data were quantified using ImageJ software. Signal intensity of the proteins of interest was normalized to the β -actin signal intensity. For validation of

anti-THBS1 and anti-SERPINA3 primary antibodies, recombinant mouse THBS1 (catalogue number 7859-TH-050) and SERPINA3 (catalogue number 4709-PI-010) proteins were used as positive controls, which were purchased from Bio-Techne (Dublin, Ireland).

2.7 Histology

Aortic segments were fixed in 4% formalin for 24 h, dehydrated overnight in 60% isopropanol, and then embedded in paraffin. Transversal sections (5 μ m) were stained with sirius red or orcein to determine total collagen and elastin content. Images were acquired with Universal Graph 6.1 software using an Olympus BX40 microscope and quantified with ImageJ software. Total collagen and elastin content were quantified by calculating the signal-to-wall area ratio (expressed as percentage).

2.8 Proteomics

Aortic samples (two segments of 2 mm each) were collected in 5 M urea and 50 mM ammonium bicarbonate (ABC) in 1.5 mL Eppendorf tubes. Cell lysis was performed using a bead beater, followed by three freeze–thaw cycles, using a -80°C freezer for freezing and sonicating in an ultrasonic bath for thawing. Undissolved particles were removed by centrifugation (30 min; 15,000 g; 4°C), and proteins in solution were transferred to new tubes. Protein samples were reduced with dithiothreitol (DTT; 20 mM) for 45 min and alkylated with iodoacetamide (IAM; 40 mM) for 45 min in the dark. The alkylation was terminated by adding an additional 20 mM DTT to consume any excess IAM. Next, protein digestion was performed with a mixture of LysC and trypsin, which was added at a ratio of 1:25 (enzyme to protein). After 2 h of digestion at 37°C in a thermoshaker at 750 rpm, the lysate was diluted with ABC (50 mM) to 1 M urea and further digested overnight in the thermoshaker. The digestion was terminated by addition of formic acid (FA) to a total of 1%. Peptide separation was subsequently performed on a Thermo Scientific (Dionex) Ultimate 3000 Rapid Separation ultra-high-performance liquid chromatography (UHPLC) system equipped with a PepSep C18 analytical column (15 cm, ID 75 μ m, 1.9 μ m Reprosil, 120 \AA). Peptide samples were first de-salted on an online installed C18 trapping column. After de-salting, peptides were separated on the analytical column with a 90-min linear gradient from 5 to 35% acetonitrile (©) with 0.1% FA at 300 nL/min flow rate. The UHPLC system was coupled to a Q Exactive HF mass spectrometer (Thermo Scientific) with the following settings: full MS scan between 250 and 1250 m/z at resolution of 120 000 followed by MS/MS scans of the top 15 most intense ions at a resolution of 15 000.

For protein identification and quantitation, the data-dependent acquisition spectra were analysed with Proteome Discoverer (PD) version 2.2. Within the PD software, the search engine Sequest was used with the SwissProt protein database *Mus musculus* (SwissProt TaxID = 10090). The database search was performed with the following settings. Enzyme was trypsin, with a maximum of two missed cleavages, minimum peptide length of 6, precursor mass tolerance of 10 ppm, fragment mass tolerance of 0.02 Da, dynamic modifications of methionine oxidation and protein N-terminus acetylation, and static modification of cysteine carbamidomethylation. Protein quantitation was performed by using default label-free quantification (LFQ) settings in PD 2.2. In short, for peptide abundancies, the peptide precursor intensities were used, and normalization was performed on total peptide amount. Protein ratios were calculated as the median of all possible pairwise peptide ratios (compared with vehicle) between biological replicates, and background-based ANOVA hypothesis testing was used to ascertain which proteins were significantly differentially expressed. PD uses a background-based ANOVA method to calculate adjusted (adj.) *P*-values to determine whether a protein is differentially expressed compared with a so-called 'background' population of proteins, as described by Navarro et al.²⁹ In principle, the algorithm first establishes a distribution of all proteins with similar abundance and abundance ratios, i.e. 'background', and calculates a median abundance ratio and confidence interval for this background population. The background population is determined for each protein of interest individually depending on its absolute abundance (i.e. high-abundant proteins of interest are compared with

high-abundant background proteins and low-abundant proteins of interest to low-abundant background proteins). In the next step, the algorithm assumes that the protein of interest has a similar confidence interval and considers this protein as differentially expressed when confidence intervals do not overlap. Finally, for multiple testing, Benjamini–Hochberg correction is performed to calculate adj. *P*-values with a false discovery rate of 5%.

2.9 Quantification of SERPINA3 and THBS1 in plasma of patients with AICT

Two cohorts of patients were enrolled, namely, cancer survivors with anthracycline-induced cardiotoxicity (AICT; $n = 14$) and control patients ($n = 27$). For the AICT population, cardiotoxicity was defined as development of LVEF below 50% during or following anthracycline treatment. Blood was collected 5 years (median) after anthracycline therapy completion. At the time of blood sampling, AICT patients exhibited a LVEF below 50%. For comparison, age-matched control patients, scheduled for diagnostic heart catheterization, were included as well. Control patients had normal cardiac function (LVEF $\geq 60\%$) and no prior history of cancer/cancer treatment. All patients received heparin during catheterization. This study was approved by the Ethical Committee of the OLV Aalst Hospital and all patients signed an informed consent.

Plasma SERPINA3 and THBS1 levels were quantified using commercially available ELISA kits (Human Alpha 1-Antichymotrypsin ELISA, Immunology Consultants Laboratory, Inc., USA, and Human Thrombospondin-1 Quantikine ELISA, Bio-Techne Ltd®, R&D Systems®, Abingdon, UK), according to the manufacturer's instructions.

2.10 Chemical compounds

PE, L-NAME, ACh, and DEANO were obtained from Sigma-Aldrich (Overijse, Belgium).

2.11 Statistical analysis

All results were expressed as the mean \pm standard error of the mean (SEM), unless stated otherwise. Statistical analyses were performed using GraphPad Software (Prism 9—Version 9.4.0; GraphPad, California, USA). A $P < 0.05$ was considered statistically significant. For proteomics, identified proteins were considered differentially expressed when the adj. *P*-value was below 0.05.

3. Results

3.1 Survival of DOX-treated mice

No mortality was observed in vehicle-treated mice, whereas seven DOX-treated mice died across the cohorts. More specifically, in Cohort 1, one DOX-treated mouse died shortly after the final *in vivo* measurement at Week 6. One mouse in the DOX-treated group of Cohort 2 died at Week 8. From Week 10 to Week 15, three DOX-treated mice died in Cohort 3. In addition, one mouse in Cohort 2 (at Week 5) and one mouse in Cohort 3 (after the *in vivo* measurement at Week 15) required euthanasia due to poor health (weight loss $>20\%$, hunched back, and lack of grooming). Mice survival for each cohort is summarized in [Supplementary material online, Figure S1](#).

3.2 DOX transiently increases *in vivo* arterial stiffness

The study design is schematically illustrated in [Figure 1A](#).

In all cohorts, DOX consistently increased aaPWV (by 1.3-fold on average) after 2 weeks of treatment, which was no longer observed at Weeks 6, 9, and 15 of follow-up ([Figure 1B](#)). Of note, DOX-induced arterial stiffness reverted to baseline before the end of the treatment period (at Week 4; [Figure 1B](#); Cohort 1). Furthermore, LVEF decreased by 10% on average in the DOX group at Week 6 in all cohorts, which tended to persist at

Week 9 and 15 (Figure 1C). Pearson correlation between aaPWV at Week 2 and LVEF at Week 6 for all cohorts showed an inverse correlation (Figure 1D). Additional parameters of cardiac function are summarized in Table 1, which show lower FS in the DOX-treated group at Weeks 6, 9, and 15. Finally, systolic BP and diastolic BP, which were only assessed in Cohort 3, were not changed during and after DOX treatment (Figure 1E). Pulse pressure, the difference between systolic and diastolic BP, remained unaffected as well (data not shown).

Next, *ex vivo* experiments were performed with the in-house developed ROTSAC set-up, which allows for evaluation of *ex vivo* arterial stiffness in the absence of possible haemodynamic confounders. Of note, the 'Week 2' data have previously been published but are shown here to allow for comparison with other time points.²⁵ *Ep* was measured at 80–120 mmHg for all conditions. Under unstimulated Krebs conditions, *Ep* was not altered (Figure 2A). On the other hand, DOX increased *Ep* in the presence of PE at Week 2, which was no longer observed at Weeks 6, 9, and 15 (Figure 2B). This is in line with the *in vivo* measurements. Finally, *Ep* values were similar between vehicle- and DOX-treated groups under DEANO (Figure 2C).

3.3 DOX impairs endothelium-dependent vasodilation that eventually recovers

Vascular reactivity was subsequently examined in depth. Endothelium-dependent vasodilation with ACh was decreased in the DOX-treated group at Week 6, which was no longer observed at Weeks 9 and 15 (Figure 3A). Endothelium-independent relaxation with DEANO was not altered at any time point (Figure 3B).

PE-induced contraction was higher at Weeks 6 and 9 (Figure 4A). When contraction in Panel A was normalized to maximum contraction, aortic segments from DOX-treated mice exhibited increased sensitivity of contraction at Weeks 6, 9, and 15 (Figure 4B). Next, PE-induced contraction, after prior incubation of aortic segments with the eNOS inhibitor L-NAME, was only higher in DOX-treated mice at Week 9 (Figure 4C). Normalized contraction from Panel C was identical at Weeks 6, 9, and 15 (Figure 4D).

3.4 DOX does not alter collagen and elastin content nor induces outward structural remodelling

Next, we investigated the occurrence of structural changes in the aortic wall to elucidate why DOX-induced arterial stiffness was no longer present at Week 6 despite persistent endothelial dysfunction. Total collagen and elastin content, histologically stained with sirius red and orcein respectively, were similar between the vehicle- and DOX-treated groups (see Supplementary material online, Figure S2). Furthermore, aortic diameters, assessed with the ROTSAC set-up under DEANO, did not differ. More specifically, diameters were as follows for the vehicle vs. DOX group: 0.94 ± 0.01 vs. 0.96 ± 0.02 mm at Week 2, 1.01 ± 0.04 vs. 0.97 ± 0.02 mm at Week 6, 1.07 ± 0.04 vs. 1.06 ± 0.03 mm at Week 9, and 1.01 ± 0.01 vs. 1.01 ± 0.06 mm at Week 15.

3.5 DOX increases THBS1 and SERPINA3 levels during treatment

Proteomic analysis of aortic samples identified a total of 966 proteins (755 with high and 211 with medium confidence), of which 37 were differentially expressed (28 up-regulated and 9 down-regulated) at Week 2. At Week 6, 25 proteins were differentially expressed (15 up-regulated and 10 down-regulated). The results are visually summarized in Figure 5A. A more detailed list of the differentially up- and down-regulated proteins is provided in a supplementary Excel® file.

Thrombospondin-1 (THBS1) and α -1-antichymotrypsin orthologue 'n' (SERPINA3N; hereafter called 'SERPINA3') showed the highest expression levels at Weeks 2 and 6, respectively. We further validated the differential expression of these proteins using western blotting and investigated

whether the up-regulation persisted at Week 9. For DOX-treated mice, western blotting revealed increased SERPINA3 at Weeks 2 and 6 (Figure 5B). The elevated SERPINA3 levels at Week 6 corroborate the proteomic findings. SERPINA3 levels remained higher at Week 9 (Figure 5B). Furthermore, in the DOX group, increased expression of THBS1 at Weeks 2 and 6 was observed, which is in line with the proteomic results (Figure 5B). THBS1 tended to remain high at Week 9 ($P = 0.052$; Figure 5B). For each time point, western blot images for SERPINA3 and THBS1 are shown in Figure 5C. Uncropped blots are shown in the supplementary PDF file. The specificity of anti-SERPINA3 and anti-THBS1 antibodies was validated with recombinant mouse SERPINA3 and THBS1 proteins as positive controls. The antibody specificity validation is shown in Supplementary material online, Figure S3.

3.6 SERPINA3 and THBS1 increase in plasma of patients with AICT

The up-regulation of SERPINA3 and THBS1 places these proteins as potential biomarkers for DOX-induced cardiovascular toxicity. As such, SERPINA3 and THBS1 levels were quantified in plasma samples from AICT and control patients.

An overview of the patient cohorts is illustrated in Figure 6A. Patient characteristics are summarized in Table 2 and were as follows: AICT patients ($n = 14$) were aged 59 years (median; range: 41–75 years), and 12 patients (86%) were female. AICT patients were treated for breast cancer ($n = 11$), T-cell lymphoma ($n = 1$), non-Hodgkin lymphoma ($n = 1$), or Hodgkin lymphoma ($n = 1$). For AICT patients, median LVEF was 36% (range: 14–41%) at the time of blood collection. Noteworthy, 12 patients (86%) showed severe cardiotoxicity (LVEF < 40%) as defined by the current ESC guidelines on cardio-oncology,²² and 2 patients (14%) exhibited a LVEF of 40–41%. Furthermore, hypertension and hypercholesterolaemia were observed in one AICT patient (7%) and seven AICT patients (50%), respectively. None of the AICT patients had diabetes. For the control group ($n = 27$), patients were aged 57 years (median; range: 48–78 years), 15 (56%) were female, 11 patients (41%) exhibited hypertension, 11 (41%) showed hypercholesterolaemia, and 3 (11%) had diabetes. In control patients, median LVEF was 73% (range: 60–88%) at the time of blood collection.

SERPINA3 and THBS1 were both detected in plasma, indicating that these proteins are secreted, and were significantly higher in the AICT group compared with control patients (Figure 6B). No differences were observed in SERPINA3 and THBS1 levels between male and female control patients (data not shown). Pearson correlation showed an inverse correlation between SERPINA3 and LVEF and between THBS1 and LVEF (Figure 6C).

4. Discussion

The present study is, to the best of our knowledge, the first to characterize the time course of DOX-induced cardiovascular toxicity, complemented by a biomarker-oriented proteomic approach.

DOX enhanced arterial stiffness by 1.3-fold and decreased LVEF and FS by 10%. This is in line with clinical trials that have reported a 1.2-fold increase in arterial stiffness and a 10% decline in LVEF in cancer patients receiving DOX every 14–21 days (cumulative dose range: 50–400 mg/m²).^{13–17} Hence, the experimental model has translational value. Of note, a decrease of 10% in LVEF is defined as moderate cardiotoxicity in current ESC guidelines.²² Early identification of moderate cardiotoxicity is important to allow timely intervention before it turns symptomatic and/or irreversible.²² In light of this growing awareness, our DOX dosing and treatment regimen were designed accordingly and were based on a study by Zhang *et al.*³⁰ that reported a 10% decrease in LVEF during DOX treatment.

Interestingly, DOX-induced arterial stiffness preceded moderate cardiotoxicity. Additionally, there was an inverse correlation between DOX-induced arterial stiffness after 2 weeks and LVEF decline at Week 6.

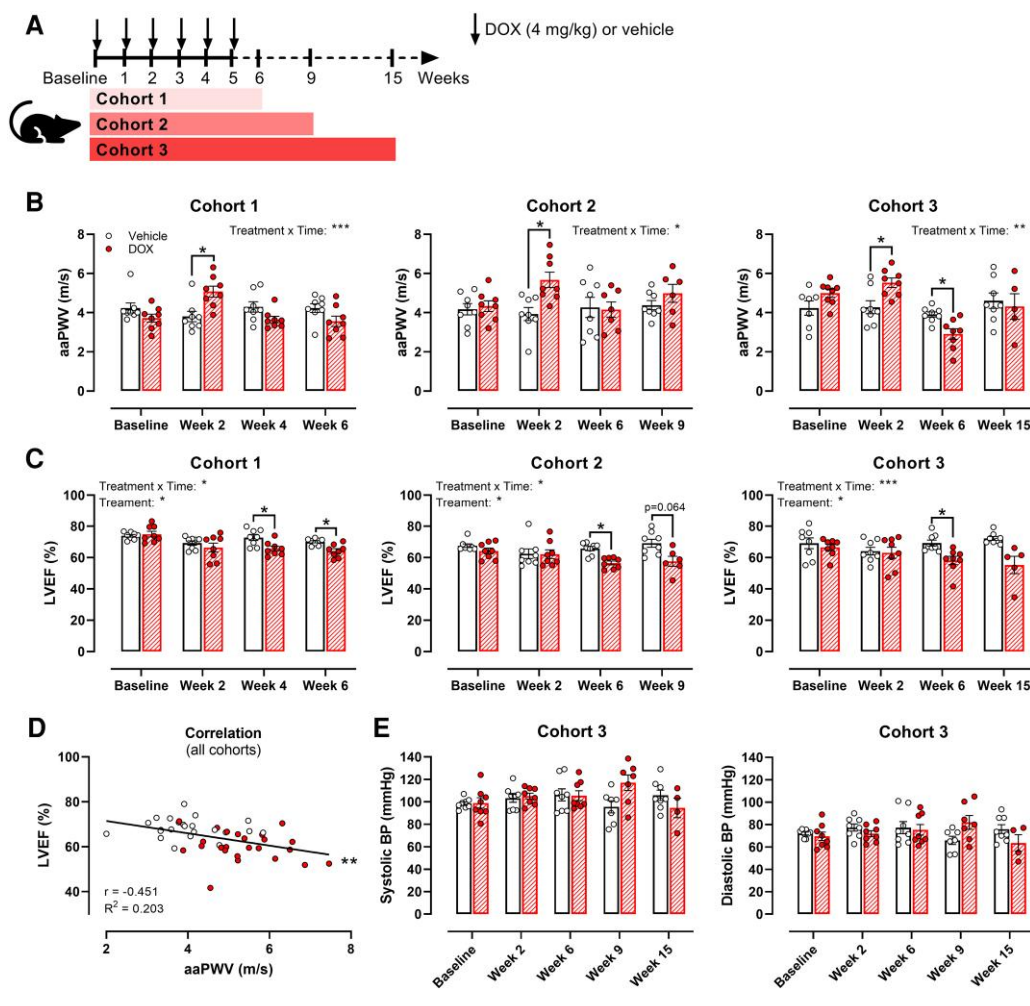


Figure 1 Evaluation of *in vivo* cardiovascular function during and after DOX treatment in each cohort. Schematic overview of the study design with full and dotted lines representing treatment and follow-up period, respectively (A). In each cohort, DOX increased aPWV after 2 weeks of treatment, followed by a return to baseline during follow-up (B). DOX consistently and persistently decreased LVEF in all cohorts (C). LVEF at Week 6 showed an inverse correlation with aPWV at Week 2 (D). Systolic and diastolic BP did not change during and after DOX treatment (E). For B, C, and E, repeated measures two-way ANOVA with Šidák's multiple comparisons test. For each cohort at baseline, $n = 8$ in vehicle- and DOX-treated group. *, **, and *** $P < 0.05$, 0.01 , and 0.001 .

Although these data do not evince a direct contributory role for DOX-induced arterial stiffness to cardiac dysfunction, our data place arterial stiffness as a potential diagnostic marker of future cardiac events in DOX-treated patients.

Decreased left ventricular systolic function persisted after DOX therapy cessation, whereas enhanced arterial stiffness recovered rapidly during the treatment period. To corroborate the latter finding, the *ex vivo* ROTSAC set-up was used to assess arterial stiffness in the absence of possible *in vivo* haemodynamic confounders since cardiac function can influence vascular stiffness.³¹ The ROTSAC set-up confirmed the *in vivo* measurements, as evidenced by increased *ex vivo* arterial stiffness at Week 2 (under PE conditions), followed by recovery during follow-up. Taken together, these findings indicate that DOX-induced arterial stiffness is transient and reverts independently from *in vivo* haemodynamics.

Our pre-clinical findings showing recovery of DOX-induced arterial stiffness are in line with the observations of Novo *et al.*¹⁶ in patients. In their clinical trial, the authors reported enhanced arterial stiffness in breast cancer patients upon DOX therapy completion, followed by recovery at 3 and 9 months after treatment end, while LVEF was lower at all time points.¹⁶ Furthermore, temporary DOX-induced arterial stiffness has been

indirectly observed in DOX-treated non-human primates as well.³² More specifically, Engwall *et al.*³² treated these primates with DOX over a period of 19 weeks (cumulative DOX dose of 11–17 mg/kg) and reported that pulse pressure increased after 2 weeks and subsequently decreased in the DOX group. Since pulse pressure has been proportionally associated with arterial stiffness,³³ its biphasic response in the study by Engwall *et al.* is indicative of transient arterial stiffness.

In the current work, we did not discern changes in either BP or pulse pressure during DOX treatment. This differs from epidemiological studies reporting a higher incidence of systemic hypertension in 5-year anthracycline-treated childhood cancer survivors.⁶ It should be mentioned that the experimental design in the current work shows a shorter time frame compared with the 5-year follow-up period in these cancer survivors. Furthermore, our unchanged BP data also differ from Engwall *et al.*³² reporting a decrease in BP in DOX-treated non-human primates. This is most likely attributable to different BP assessment methodology. While Engwall *et al.*³² evaluated central BP by using telemetry in primates at rest, we assessed peripheral BP with a tail-cuff system in restrained mice. Collectively, these studies indicate that the impact of DOX on BP remains poorly understood.

Table 1 Cardiac function and body weight at baseline and time point of sacrifice for each cohort

	Cohort 1		Cohort 2		Cohort 3	
	Baseline vehicle (n = 8) vs. DOX (n = 8)	Week 6 vehicle (n = 8) vs. DOX (n = 7)	Baseline vehicle (n = 8) vs. DOX (n = 8)	Week 9 vehicle (n = 8) vs. DOX (n = 6)	Baseline vehicle (n = 8) vs. DOX (n = 8)	Week 15 vehicle (n = 8) vs. DOX (n = 5)
FS (%)	41.5 ± 0.7 vs. 42.7 ± 1.6	38.9 ± 0.5 vs. 33.9 ± 0.8**	36.9 ± 1.0 vs. 34.5 ± 1.4	38.3 ± 2.2 vs. 29.9 ± 2.1**	37.9 ± 2.8 vs. 35.9 ± 1.4	40.7 ± 1.1 vs. 28.6 ± 3.3**
LVAW (mm; diastole)	0.73 ± 0.04 vs. 0.73 ± 0.02	0.77 ± 0.03 vs. 0.71 ± 0.02	0.80 ± 0.04 vs. 0.80 ± 0.04	0.85 ± 0.05 vs. 0.70 ± 0.05	1.03 ± 0.06 vs. 0.93 ± 0.10	0.85 ± 0.04 vs. 0.71 ± 0.03
LVAW (mm; systole)	1.09 ± 0.04 vs. 1.13 ± 0.04	1.18 ± 0.02 vs. 1.04 ± 0.03*	1.2 ± 0.05 vs. 1.1 ± 0.06	1.25 ± 0.06 vs. 0.97 ± 0.07**	1.59 ± 0.07 vs. 1.49 ± 0.09	1.24 ± 0.06 vs. 0.99 ± 0.04 [#]
LVPW (mm; diastole)	0.83 ± 0.03 vs. 0.85 ± 0.03	0.88 ± 0.06 vs. 0.83 ± 0.04	0.71 ± 0.02 vs. 1.01 ± 0.25	0.75 ± 0.04 vs. 0.79 ± 0.03	1.19 ± 0.08 vs. 1.07 ± 0.06	0.95 ± 0.02 vs. 1.00 ± 0.13
LVPW (mm; systole)	1.42 ± 0.05 vs. 1.43 ± 0.07	1.42 ± 0.05 vs. 1.25 ± 0.03*	1.25 ± 0.07 vs. 1.24 ± 0.02	1.24 ± 0.05 vs. 1.13 ± 0.05	1.53 ± 0.11 vs. 1.43 ± 0.08	1.58 ± 0.05 vs. 1.27 ± 0.17
LVID (mm; diastole)	3.04 ± 0.17 vs. 3.16 ± 0.10	3.68 ± 0.08 vs. 3.38 ± 0.04	3.68 ± 0.08 vs. 3.70 ± 0.07	3.77 ± 0.10 vs. 3.70 ± 0.12	2.95 ± 0.13 vs. 3.34 ± 0.17	3.64 ± 0.09 vs. 3.87 ± 0.32
LVID (mm; systole)	1.78 ± 0.10 vs. 1.81 ± 0.09	2.25 ± 0.06 vs. 2.23 ± 0.04	2.32 ± 0.05 vs. 2.42 ± 0.08	2.33 ± 0.12 vs. 2.59 ± 0.11	1.82 ± 0.10 vs. 2.14 ± 0.11	2.16 ± 0.09 vs. 2.80 ± 0.37*
Heart mass (mg)	N.A.	154.8 ± 5.2 vs. 128.1 ± 3.7**	N.A.	160.2 ± 8.6 vs. 154.0 ± 8.1	N.A.	136.3 ± 11.6 vs. 152.0 ± 11.6
Body weight (mg)	28.6 ± 0.6 vs. 28.3 ± 0.5	30.4 ± 0.6 vs. 26.5 ± 0.8***	25.1 ± 0.7 vs. 26.0 ± 0.6	30.7 ± 1.0 vs. 26.2 ± 1.1**	25.5 ± 0.8 vs. 25.0 ± 0.6	30.5 ± 0.9 vs. 26.1 ± 1.2**

For each cohort, repeated measures two-way ANOVA with Šidák's multiple comparisons test. Asterisk indicates statistical significant outcome from multiple comparisons test *, **, *** $P < 0.05$, 0.01, 0.001; [#] $0.05 < P < 0.06$.

FS, fractional shortening; LVAW, left ventricular anterior wall; LVPW, left ventricular posterior wall; LVID, left ventricular internal diameter; N.A., not applicable.

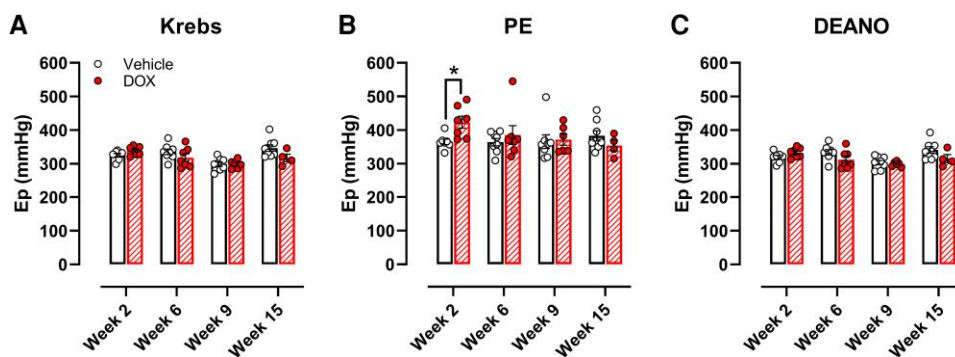


Figure 2 Assessment of *ex vivo* arterial stiffness in aortic segments isolated from vehicle- and DOX-treated mice in *ex vivo* ROTSAC set-up. Ep did not differ in Krebs (A). Ep was higher in the DOX-treated group upon PE-induced contraction at Week 2 and returned to baseline during follow-up (B). Under DEANO conditions, Ep was not altered (C). For each panel, repeated measures two-way ANOVA with Šidák's multiple comparisons test. For vehicle, $n = 8$ at each time point. For DOX-treated group, $n = 7$ at Weeks 2 and 6, $n = 6$ at Week 9, and $n = 4$ at Week 15.

Although our results show recovery of DOX-induced arterial stiffness, this does not necessarily mean reversal of vascular toxicity. Arterial stiffness is modulated by passive biomechanical properties, such as the collagen-to-elastin ratio,³⁴ by active processes, such as the regulation of vascular tone by VSMCs and ECs,^{27,35} and by the mutual interplay between these passive and active elements.³⁴ As such, multiple vascular events could collectively exert opposing actions on arterial stiffness. For example, in the acute phase (16-h treatment with 4-mg DOX/kg *in vivo*), we previously observed impaired endothelial function and reduced VSMC contraction,

exerting mutual opposing effects, which eventually resulted in unaltered arterial stiffness.³⁶ This highlights the importance of evaluating both active and passive mechanisms to obtain a complete profile of vascular toxicity.

In-depth vascular reactivity evaluation revealed important findings. Previously, we demonstrated that the increase in *in vivo* and *ex vivo* arterial stiffness during the first 2 weeks of DOX treatment resulted from endothelial dysfunction, as evidenced by impaired ACh-stimulated vasodilation and a decreased basal NO index.²⁵ In the present work, ACh-induced vasodilation in the DOX-treated group remained impaired at Week 6

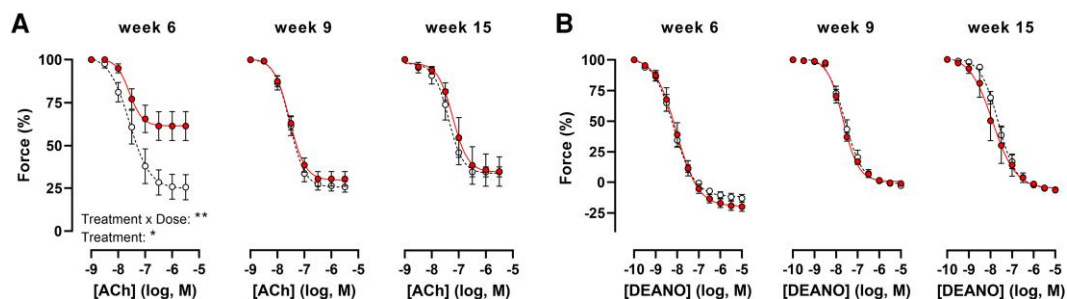


Figure 3 Endothelium-dependent (ACh; A) and endothelium-independent (DEANO; B) vasodilation in aortic segments from vehicle- and DOX-treated mice in organ baths. DOX impaired ACh-induced vasodilation at Week 6, which recovered thereafter (A). DOX did not affect DEANO-induced vasodilation at any time point (B). For vehicle, $n = 8$ for each time point; for DOX-treated group, $n = 7$ at Week 6, $n = 6$ at Week 9 and $n = 4$ at Week 15. For each time point in each panel, repeated measures two-way ANOVA with Šidák's multiple comparisons test. * and ** $P < 0.05$ and 0.01 .

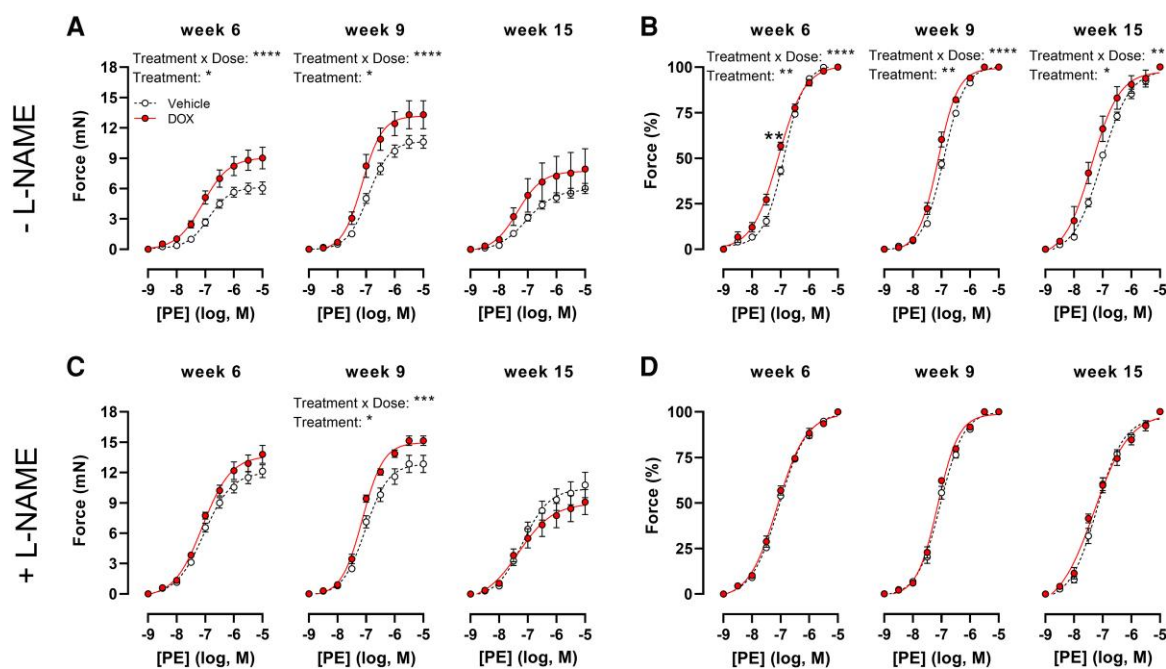


Figure 4 PE-induced VSMC contraction in aortic segments from vehicle- and DOX-treated mice in organ baths. DOX increased PE-induced contraction at Weeks 6 and 9 (A). Normalization of A to maximum contraction revealed higher contraction in the DOX-treated group at all time points (B). PE-induced contraction after pre-incubation with L-NAME was higher in DOX-treated mice at Week 9 (C). Normalization of C to maximum contraction revealed similar contraction at all time points (D). For vehicle, $n = 8$ for each time point; for DOX-treated group, $n = 7$ at Week 6, $n = 6$ at Week 9, and $n = 4$ at Week 15. For each time point in each panel, repeated measures two-way ANOVA with Šidák's multiple comparisons test. *, **, ***, and **** $P < 0.05$, 0.01 , 0.001 and 0.0001 .

but restored at Weeks 9 and 15. As such, the reversibility of DOX-induced arterial stiffness does not seem attributable to endothelial dysfunction recovery. Surprisingly, PE-induced contraction remained higher during follow-up in the absence, but not in the presence, of L-NAME. We previously reported that such observation is indicative of low basal NO levels.^{27,28} Likewise, decreased basal NO levels and similar ACh-induced vasodilation have been reported in atherosclerotic mouse models with endothelial dysfunction.^{37,38} Therefore, DOX-induced endothelial dysfunction may only partially restore after therapy cessation, but these

data should be interpreted with caution as basal NO levels were not directly measured nor quantified. In any event, our data indicate that, as long as DOX treatment continues, ACh-stimulated vasodilation and basal NO levels remain impaired.

We previously demonstrated that DOX (4 mg/kg) provoked endothelial dysfunction as early as 16 h after administration, without affecting arterial stiffness or cardiac function.³⁶ In the present study, DOX increased arterial stiffness after 2 weeks and decreased LVEF from Week 4. Taken together, DOX provokes endothelial dysfunction soon after administration, which

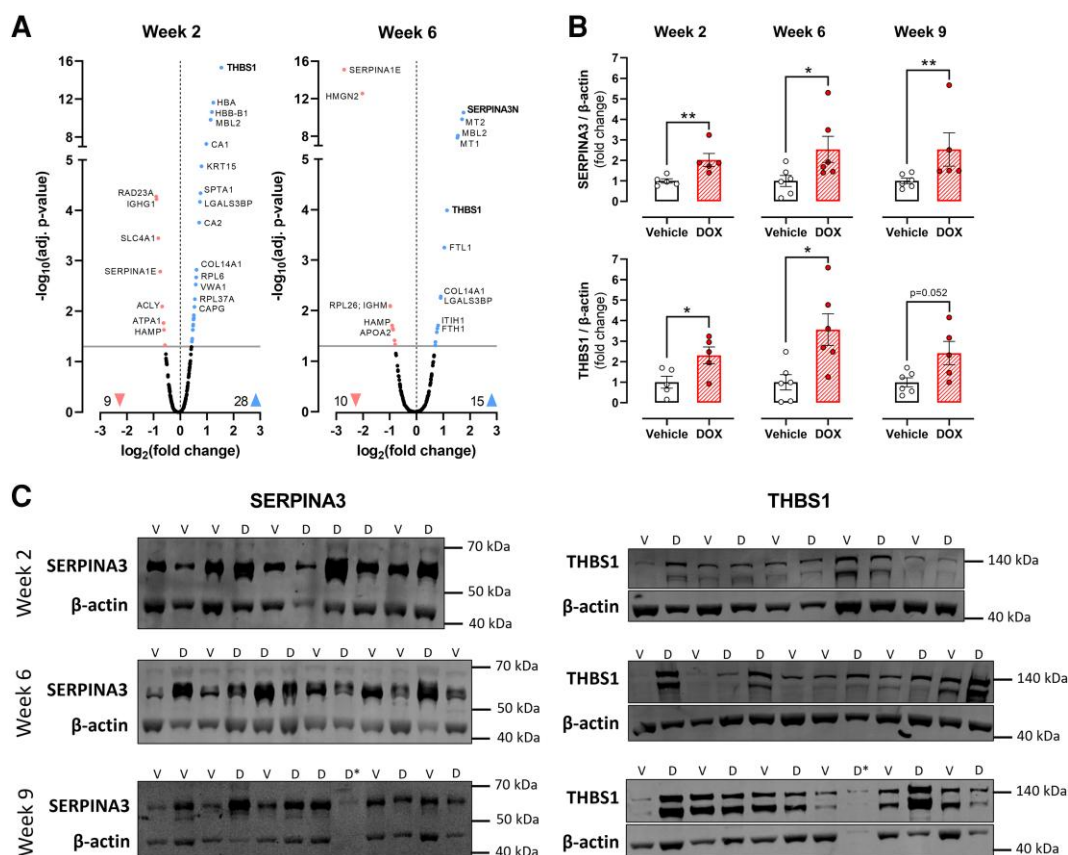


Figure 5 Proteomic analysis of aortic samples from DOX-treated mice at Weeks 2 and 6 and validation of two candidate biomarkers with western blotting. Plots of differentially expressed proteins at Weeks 2 and 6 (A). For A, horizontal grey line indicates significance threshold ($P < 0.05$); up- and down-regulated proteins are indicated in blue and red, respectively; differentially expressed proteins are abbreviated (full names are listed in abbreviations list). Western blotting shows and corroborates higher levels of SERPINA3 in DOX-treated mice at Weeks 2 and 6, which persist at Week 9 (B). Western blotting also confirms higher levels of THBS1 in the DOX-treated group at Weeks 2 and 6 and shows a trend ($P = 0.052$) towards increased THBS1 levels at Week 9 (B). Representative western blot images for SERPINA3 and THBS1 at Weeks 2, 6, and 9 (C). For C, 'V' and 'D' indicate lanes with vehicle and DOX aortic samples, respectively. D* on the blot at Week 9 contains a DOX sample for which no protein was detected and was excluded from analysis as such. For A, $n = 8$ in vehicle and DOX group for both Week 2 and Week 6. For B, vehicle group: $n = 5$, $n = 6$, and $n = 6$ at Weeks 2, 6, and 9, respectively; DOX group: $n = 5$, $n = 6$, and $n = 5$ at Weeks 2, 6, and 9, respectively. For B, Mann–Whitney U test for each time point. * and ** $P < 0.05$ and 0.01 . **Abbreviations for differentially expressed proteins in proteomics:** SERPINA1E, α -1-antitrypsin; HMG2, Non-histone chromosomal protein HMG-17; SERPINA3N, α -1-antichymotrypsin orthologue n; MT2, Metallothionein-2; MBL2, Mannose-binding protein C; MT1, Metallothionein-1; THBS1, Thrombospondin-1; FTL1, Ferritin light chain 1; COL14A1, Collagen α -1 (XIV) chain; LGALS3BP, Galectin-3-binding protein; RPL26, 60S ribosomal protein L26; IGHM, Immunoglobulin heavy constant μ ; HAMP, Hepcidin; APOA2, Apolipoprotein A-II; HBA, Hemoglobin subunit α ; HBB-B1, Hemoglobin subunit β -1; CA1, Carbonic anhydrase 1; KRT15, Keratin (type I cytoskeletal 15); SPTA1, Spectrin α ; CA2, Carbonic anhydrase 2; RPL6, 60S ribosomal protein L6; VWA1, von Willebrand factor A domain-containing protein 1; RPL37A, 60S ribosomal protein L37a; CAPG, Macrophage-capping protein; RAD23A, UV excision repair protein RAD23 homolog A; IGHG1, Ig γ -1 chain C region (membrane-bound form); SLC4A1, Band 3 anion transport protein; ACLY, ATP-citrate synthase; ATPA1, Sodium/potassium-transporting ATPase subunit alpha-1.

precedes both arterial stiffness and moderate cardiotoxicity. In this respect, endothelial dysfunction may be an early indicator of future cardiovascular events in cancer patients during DOX therapy.

In an attempt to explain arterial stiffness recovery despite continued endothelial dysfunction (at Week 6), we investigated whether structural remodelling was the discriminating factor. Sirius red and orcein stains showed similar amounts of collagen and elastin, and *ex vivo* arterial stiffness under DEANO did not differ. In addition, no outward remodelling occurred, as suggested by similar aortic diameters. However, proteomics on aortic samples revealed differential expression of particularly glycoproteins, such as THBS1, SERPINA3, SERPINA1, MBL2, and LGALS3BP. While these glycoproteins mediate cell–cell and cell–extracellular matrix interactions (GeneCards®; accessed on 12 April 2023), their exact role in vascular

physiology and arterial stiffness remains incompletely understood. Further investigating this lies beyond the scope of the current work. Of note, SERPINA3 and THBS1 represented the highest up-regulated proteins in response to DOX. Western blotting further confirmed the up-regulated expression and showed that both SERPINA3 and THBS1 levels remained higher after DOX therapy cessation. As such, SERPINA3 and THBS1 were selected as promising biomarker candidates for clinical validation.

Plasma SERPINA3 and THBS1 levels were higher in middle-aged AICT cancer survivors compared with control patients. Moreover, there was an inverse correlation between SERPINA3 and LVEF and between THBS1 and LVEF.

SERPINA3 is a serine protease inhibitor, involved in acute-phase inflammatory responses,³⁹ and has been implicated in Alzheimer's disease and

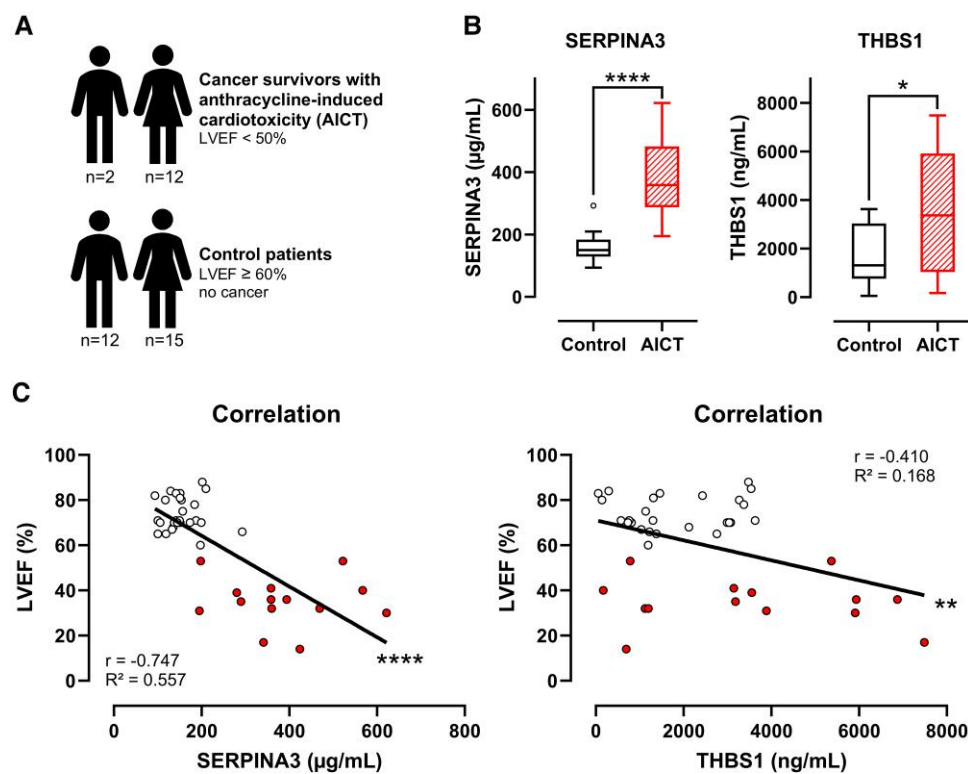


Figure 6 Quantification of SERPINA3 and THBS1 levels in plasma of control and AICT patients using ELISA. Schematic overview of the patient cohorts (A). AICT patients exhibited higher SERPINA3 and THBS1 levels compared with the control group (B). Both SERPINA3 and THBS1 showed an inverse Pearson correlation with LVEF (C). For B, data are presented as Tukey box plots with median (horizontal line) and the 25th and 75th percentile whiskers. For C, white and red dots represent control and AICT patients, respectively. *n* numbers are shown in A. For B, Mann–Whitney *U* test. * and **** *P* < 0.05 and 0.0001.

Table 2 Patient cohort characteristics

	AICT patients	Control patients
Population (<i>n</i>)	14	27
Age (years; median)	59	57
Proportion of females (%)	86	56
Cancer type		
Breast cancer (<i>n</i>)	11	None
T-cell lymphoma (<i>n</i>)	1	None
Non-Hodgkin lymphoma (<i>n</i>)	1	None
Hodgkin lymphoma (<i>n</i>)	1	None
LVEF (%; median)	36	73
Patients with hypertension (<i>n</i>)	1	11
Patients with hypercholesterolaemia (<i>n</i>)	7	11
Patients with diabetes (<i>n</i>)	None	3

various types of cancer, such as breast and colorectal cancers.^{39–41} In recent years, SERPINA3 has been proposed as a prognostic marker for cardiovascular disease.^{42–46} More specifically, Zhao *et al.*⁴⁶ suggested that SERPINA3 predicts adverse cardiac events in patients with myocardial infarction. Similarly, Delrue *et al.*⁴³ reported circulating SERPINA3 to be associated with worse outcome in patients with *de novo* or worsened HF. Finally, SERPINA3 has also been shown to be increased in plasma of

patients with coronary heart disease.⁴⁵ Despite its association with adverse cardiovascular outcome, it remains unclear whether SERPINA3 actively contributes to cardiovascular disease development or whether it is released as a general response to toxic events. Also, the role of SERPINA3 in normal cardiovascular physiology is poorly understood.³⁹ In any event, the present study is the first to demonstrate that DOX treatment is associated with increased SERPINA3 in the vasculature and to find up-regulated SERPINA3 in plasma of AICT patients. Our data therefore raise awareness for a role of SERPINA3 in cardiovascular toxicity and place SERPINA3 as a potential diagnostic biomarker for anthracycline-induced cardiovascular toxicity.

THBS1 is a secretory extracellular matrix protein and primarily mediates cell-to-cell and cell-to-matrix interactions. It has been shown that THBS1 can prevent vascular endothelial growth factor-mediated eNOS and guanylate cyclase activation, which could be an explanation why impaired basal NO production possibly persists after DOX therapy cessation and thus may explain the higher PE contractions.⁴⁷ Apart from inhibiting eNOS, THBS1 has been proposed to fulfil a protective role in the cardiovascular system as THBS1 deficiency in rodent models deleteriously impacts cardiovascular physiology.⁴⁸ For example, THBS1 deficiency has been observed to provoke early onset of cardiac hypertrophy following pressure overload,⁴⁹ prolong and enhance inflammatory responses after myocardial infarction,⁵⁰ and accelerate atherosclerotic plaque maturation.⁵¹ In rodent models of HF, THBS1 has also been shown to be up-regulated, presumably in an adaptive attempt to maintain cardiac function by promoting cardiac remodelling.^{52,53} As such, increased THBS1 levels have been proposed as indicators of future HF.⁵³ To our knowledge, the current work is the first to show increased plasma THBS1 levels in AICT patients. Whether THBS1 is up-regulated in

response to HF remains unclear but highlights this protein as a possible indicator of future cardiac events in patients receiving DOX.

Apart from SERPINA3 and THBS1, proteomics showed elevated MBL2 and LGALS3BP levels, which have been implicated in cardiovascular disease as well. For example, increased MBL2 levels in serum have been associated with development of coronary artery disease.⁵⁴ Moreover, LGALS3BP over-expression and secretion have been proposed to play an important part in HF and atherosclerosis.⁵⁵ Interestingly, we observed a decrease in SERPINA1, which has been associated with a higher incidence of systemic hypertension, chronic HF, and cardiac arrhythmia.⁵⁶ Similar to SERPINA3 and THBS1, the exact role of MBL2, LGALS3BP, and SERPINA1 in cardiovascular (patho)physiology remains incompletely understood.

In summary, left ventricular systolic function was persistently reduced in DOX-treated mice, whereas arterial stiffness and endothelial dysfunction were transient. Interestingly, arterial stiffness preceded impairment of systolic function and showed an inverse correlation with LVEF decline. Moreover, endothelial dysfunction manifested prior to arterial stiffness and reduced LVEF and persisted during the DOX treatment period. Hence, we propose that arterial stiffness and endothelial dysfunction hold potential as diagnostic, but time-sensitive, functional markers of future cardiovascular events in patients receiving DOX. Furthermore, we identified SERPINA3 and THBS1 up-regulation in murine aortic tissue during DOX treatment. In AICT patients, plasma SERPINA3 and THBS1 levels were elevated as well, highlighting these proteins as potential contributors or response proteins to cardiotoxicity. As such, SERPINA3 and THBS1 hold possible diagnostic value for cardiovascular risk assessment in adult DOX-treated patients.

4.1 Limitations

The present study has several limitations. First, our findings apply to young, male mice, which may differ from female and old mice. Young, male mice were chosen as they are more sensitive to DOX-induced cardiotoxicity^{57–59} and to avoid the influence of cyclic changes in female hormones as confounding factors. Similarly, female sex offers protection against DOX-related cardiotoxicity in patients.⁵⁷ Second, the DOX administration route in the current work differs from the clinical setting where DOX is mainly administered intra-venously. Third, although we position arterial stiffness and endothelial dysfunction as potential markers for cardiotoxicity in DOX-treated patients, further clinical validation is required with well-defined time points. Finally, our data only show an increase in SERPINA3 and THBS1 levels in adult AICT patients, and more research is required to investigate whether SERPINA3 and THBS1 can actually predict cardiovascular events in DOX-treated patients of all ages.

Supplementary material

Supplementary material is available at *Cardiovascular Research* online.

Authors' contributions

Conceptualization: M.B., E.V.C., and P.J.G.; methodology: M.B. and D.K.; investigation and formal analysis: M.B., D.K., C.V.A., H.B., C.N., L.D., and P.J.G.; writing—original draft preparation: M.B., E.V.C., and P.J.G.; writing, review, and editing: M.B., D.K., K.F., C.F., C.N., L.R., B.C.P., L.D., W.H., W.M., G.D.M., E.V.C., and P.J.G.; supervision: E.V.C. and P.J.G.; and funding acquisition: G.D.M., W.M., L.R., E.V.C., and P.J.G. All authors have read and agreed to the published version of the manuscript.

Acknowledgements

The authors thank Ronny Mohren from Maastricht University (the Netherlands) for technical assistance and support regarding the proteomic experiments. Graphical abstract was created with BioRender.com under publication licence.

Conflict of interest: The authors declare that they have no known competing financial interests or personal relationships that could have appeared to influence the work reported in this paper.

Funding

This work was supported by the Fund for Scientific Research (FWO) Flanders to whom M.B., K.F., C.N., and H.B. are pre-doctoral fellows (grant numbers: 1S33720N, 11C6321N, 1S24720N, and 1192420N, respectively). E.V.C. is holder of a senior clinical investigator grant from FWO Flanders (grant number: 1804320N). C.F. is holder of a clinical mandate from the Belgian Foundation against Cancer (grant number: 2021-034). L.R. is funded by the Research Council of the University of Antwerp (BOF UAntwerp ID: 45846). Furthermore, the research is supported by a DOCPRO4 grant (BOF UAntwerp ID: 39984) and by the INSPIRE project, which has received funding from the European Union's Horizon 2020 Research and Innovation Program (H2020-MSCA-ITN program, Grant Agreement: No858070).

Data availability

All data are incorporated into the article and its online [supplementary material](#).

References

- Johnson-Arbor K, Dube R. Doxorubicin. In *Statpearls*. (FL): Treasure Island; 2022.
- McGowan JV, Chung R, Maulik A, Piotrowska I, Walker JM, Yellon DM. Anthracycline chemotherapy and cardiotoxicity. *Cardiovasc Drugs Ther* 2017;**31**(1):63–75.
- Mitry MA, Edwards JG. Doxorubicin induced heart failure: phenotype and molecular mechanisms. *Int J Cardiol Heart Vasc* 2016;**10**:17–24.
- Kremer LC, van Dalen EC, Offringa M, Voûte PA. Frequency and risk factors of anthracycline-induced clinical heart failure in children: a systematic review. *Ann Oncol* 2002;**13**(4):503–512.
- Renu K, Abilash VG, Tirupathi Pichiah PB, Arunachalam S. Molecular mechanism of doxorubicin-induced cardiomyopathy - an update. *Eur J Pharmacol* 2018;**818**:241–253.
- Armstrong GT, Oeffinger KC, Chen Y, Kawashima T, Yasui Y, Leisenring W, Stovall M, Chow EJ, Sklar CA, Mulrooney DA, Mertens AC, Border W, Durand J-B, Robison LL, Meacham LR. Modifiable risk factors and major cardiac events among adult survivors of childhood cancer. *J Clin Oncol* 2013;**31**(29):3673–3680.
- Mitchell GF, Hwang S-J, Vasan RS, Larson MG, Pencina MJ, Hamburg NM, Vita JA, Levy D, Benjamin EJ. Arterial stiffness and cardiovascular events: the Framingham Heart Study. *Circulation* 2010;**121**(4):505–511.
- Lerman A, Zeiher AM. Endothelial function: cardiac events. *Circulation* 2005;**111**(3):363–368.
- Sun HJ, Wu Z-Y, Nie X-W, Bian J-S. Role of endothelial dysfunction in cardiovascular diseases: the link between inflammation and hydrogen sulfide. *Front Pharmacol* 2019;**10**:1568.
- Maruhashi T, Soga J, Fujimura N, Idei N, Mikami S, Iwamoto Y, Iwamoto A, Kajikawa M, Matsumoto T, Oda N, Kishimoto S, Matsui S, Hashimoto H, Aibara Y, Mohamad Yusoff F, Hidaka T, Kihara Y, Chayama K, Noma K, Nakashima A, Goto C, Tomiyama H, Takase B, Kohro T, Suzuki T, Ishizu T, Ueda S, Yamazaki T, Furumoto T, Kario K, Inoue T, Koba S, Watanabe K, Takemoto Y, Hano T, Sata M, Ishibashi Y, Node K, Maemura K, Ohya Y, Furukawa T, Ito H, Ikeda H, Yamashina A, Higashi Y. Endothelial dysfunction, increased arterial stiffness, and cardiovascular risk prediction in patients with coronary artery disease: FMD-J (Flow-Mediated Dilation Japan) study. *J Am Heart Assoc* 2018;**7**(14):e008588.
- Bonarjee VVS. Arterial stiffness: a prognostic marker in coronary heart disease. Available methods and clinical application. *Front Cardiovasc Med* 2018;**5**:64.
- Boutouyrie P, Tropeano AI, Asmar R, Gautier I, Benetos A, Lacolley P, Laurent S. Aortic stiffness is an independent predictor of primary coronary events in hypertensive patients: a longitudinal study. *Hypertension* 2002;**39**(1):10–15.
- Mihalcea D, Florescu M, Bruja R, Patrascu N, Vladareanu A-M, Vinereanu D. 3D echocardiography, arterial stiffness, and biomarkers in early diagnosis and prediction of CHOP-induced cardiotoxicity in non-Hodgkin's lymphoma. *Sci Rep* 2020;**10**(1):18473.
- Drafts BC, Twomley KM, D'Agostino R, Lawrence J, Avis N, Ellis LR, Thohan V, Jordan J, Melin SA, Torti FM, Little WC, Hamilton CA, Hundley WG. Low to moderate dose anthracycline-based chemotherapy is associated with early noninvasive imaging evidence of subclinical cardiovascular disease. *JACC Cardiovasc Imaging* 2013;**6**(8):877–885.
- Chaosuwannakit N, D'Agostino R, Hamilton CA, Lane KS, Ntim WO, Lawrence J, Melin SA, Ellis LR, Torti FM, Little WC, Hundley WG. Aortic stiffness increases upon receipt of anthracycline chemotherapy. *J Clin Oncol* 2010;**28**(1):166–172.
- Novo G, Di Lisi D, Manganaro R, Manno G, Lazzara S, Immordino FA, Madaudo C, Careri S, Russo A, Incorvaia L, Zito C. Arterial stiffness: effects of anticancer drugs used for breast cancer women. *Front Physiol* 2021;**12**:661464.

17. Schneider C, González-Jaramillo N, Marcin T, Campbell KL, Suter T, Bano A, Wilhelm M, Eser P. Time-dependent effect of anthracycline-based chemotherapy on central arterial stiffness: a systematic review and meta-analysis. *Front Cardiovasc Med* 2022;**9**:873898.
18. Jang WJ, Choi DY, Jeon IS. Vascular endothelial dysfunction after anthracyclines treatment in children with acute lymphoblastic leukemia. *Korean J Pediatr* 2013;**56**(3):130–134.
19. Chow AY, Chin C, Dahl G, Rosenthal DN. Anthracyclines cause endothelial injury in pediatric cancer patients: a pilot study. *J Clin Oncol* 2006;**24**(6):925–928.
20. Armenian SH, Gelehrter SK, Vase T, Venkatramani R, Landier W, Wilson KD, Herrera C, Reichman L, Menteer J-D, Mascarenhas L, Freyer DR, Venkataraman K, Bhatia S. Screening for cardiac dysfunction in anthracycline-exposed childhood cancer survivors. *Clin Cancer Res* 2014;**20**(24):6314–6323.
21. Sawaya H, Sebag IA, Plana JC, Januzzi JJ, Ky B, Cohen V, Gosavi S, Carver JR, Wieggers SE, Martin RP, Picard MH, Gerszten RE, Halpern EF, Passeri J, Kuter I, Scherrer-Crosbie M. Early detection and prediction of cardiotoxicity in chemotherapy-treated patients. *Am J Cardiol* 2011;**107**(9):1375–1380.
22. Lyon AR, López-Fernández T, Couch LS, Asteggiano R, Aznar MC, Bergler-Klein J, Boriani G, Cardinale D, Cordoba R, Cosyns B, Cutter DJ, de Azambuja E, de Boer RA, Dent SF, Farmakis D, Gevaert SA, Gorog DA, Herrmann J, Lenihan D, Moslehi J, Moura B, Salinger SS, Stephens R, Suter TM, Szmit S, Tamargo J, Thavendiranathan P, Tocchetti CG, van der Meer P, van der Pal HJH, Lancellotti P, Thuny F, Abdelhamid M, Aboyans V, Aleman B, Alexandre J, Barac A, Borger MA, Casado-Arroyo R, Cautela J, Čelutkienė J, Cikes M, Cohen-Solal A, Dhiman K, Ederhy S, Edvardsen T, Fauchier L, Fradley M, Grapsa J, Halvorsen S, Heuser M, Humbert M, Jaarsma T, Kahan T, Konradi A, Koskinas KC, Kotecha D, Ky B, Landmesser U, Lewis BS, Linhart A, Lip GYH, Løchen M-L, Malaczynska-Rajpold K, Metra M, Mindham R, Moonen M, Neilan TG, Nielsen JC, Petronio A-S, Prescott E, Rakisheva A, Salem J-E, Savarese G, Sitges M, Berg Jt, Touyz RM, Tycinska A, Wilhelm M, Zamorano JL, Laredj N, Zelveian P, Rainer PP, Samadov F, Andruschuk U, Gerber BL, Selimović M, Kinova E, Samardzic J, Economides E, Pudil R, Nielsen KM, Kafaty TA, Vettus R, Tuohinen S, Ederhy S, Pagava Z, Rassaf T, Briasoulis A, Czuriga D, Andersen KK, Smyth Y, Iakobishvili Z, Parrini I, Rakisheva A, Pruthi EP, Mirrakhimov E, Kalejs O, Skouri H, Benlamin H, Žaladuonytė D, Iovino A, Moore AM, Bursacovschi D, Benyass A, Manintveld O, Bosevski M, Gulati G, Leszek P, Fiuza M, Jurcut R, Vasyuk Y, Foscoli M, Simic D, Slanina M, Lipar L, Martin-Garcia A, Hübner L, Kurmann R, Alayed A, Abid L, Zorkun C, Nesukay E, Manisty C, Srojdinova N, Baigent C, Abdelhamid M, Aboyans V, Antoniou S, Arbelo E, Asteggiano R, Baumbach A, Borger MA, Čelutkienė J, Cikes M, Collet J-P, Falk V, Fauchier L, Gale CP, Halvorsen S, Iung B, Jaarsma T, Konradi A, Koskinas KC, Kotecha D, Landmesser U, Lewis BS, Linhart A, Lochen M-L, Mindham R, Nielsen JC, Petersen SE, Prescott E, Rakisheva A, Sitges M, Touyz RM. 2022 ESC guidelines on cardio-oncology developed in collaboration with the European Hematology Association (EHA), the European Society for Therapeutic Radiology and Oncology (ESTRO) and the International Cardio-Oncology Society (IC-OS). *Eur Heart J* 2022;**43**(41):4229–4361.
23. Di Lascio N, Stea F, Kusmic C, Sicari R, Fata F. Non-invasive assessment of pulse wave velocity in mice by means of ultrasound images. *Atherosclerosis* 2014;**237**(1):31–37.
24. Leloup AJ, Van HCE, Kurdi A, De Moudt S, Martinet W, De Meyer GRY, Schrijvers DM, De Keulenaer GW, Franssen P. A novel set-up for the ex vivo analysis of mechanical properties of mouse aortic segments stretched at physiological pressure and frequency. *J Physiol* 2016;**594**(21):6105–6115.
25. Bosman M, Favere K, Neutel CHG, Jacobs G, De Meyer GRY, Martinet W, Van Craenenbroeck EM, Guns PJDF. Doxorubicin induces arterial stiffness: a comprehensive in vivo and ex vivo evaluation of vascular toxicity in mice. *Toxicol Lett* 2021;**346**:23–33.
26. Neutel CHG, Corradin G, Puylaert P, De Meyer GRY, Martinet W, Guns P-J. High pulsatile load decreases arterial stiffness: an ex vivo study. *Front Physiol* 2021;**12**:741346.
27. Leloup AJ, Van Hove CE, De Moudt S, De Meyer GRY, De Keulenaer GW, Franssen P. Vascular smooth muscle cell contraction and relaxation in the isolated aorta: a critical regulator of large artery compliance. *Physiol Rep* 2019;**7**(4):e13934.
28. van Langen J, Franssen P, Van Hove CE, Schrijvers DM, Martinet W, De Meyer GRY, Bult H. Selective loss of basal but not receptor-stimulated relaxation by endothelial nitric oxide synthase after isolation of the mouse aorta. *Eur J Pharmacol* 2012;**696**(1–3):111–119.
29. Navarro P, Trevisan-Herraz M, Bonzon-Kulichenko E, Núñez E, Martínez-Acedo P, Pérez-Hernández D, Jorge I, Mesa R, Calvo E, Carrascal M, Hernández ML, García F, Bárcena JA, Ashman K, Abian J, Gil C, Redondo JM, Vázquez J. General statistical framework for quantitative proteomics by stable isotope labeling. *J Proteome Res* 2014;**13**(3):1234–1247.
30. Zhang S, Liu X, Bawa-Khalfe T, Lu L-S, Lyu YL, Liu LF, Yeh ETH. Identification of the molecular basis of doxorubicin-induced cardiotoxicity. *Nat Med* 2012;**18**(11):1639–1642.
31. Obata Y, Mizogami M, Singh S, Nyhan D, Berkowitz DE, Stepan J, Barodka V. The effects of hemodynamic changes on pulse wave velocity in cardiothoracic surgical patients. *Biomed Res Int* 2016;**2016**:9640457.
32. Engwall MJ, Evers N, Turk JR, Vargas HM. The effects of repeat-dose doxorubicin on cardiovascular functional endpoints and biomarkers in the telemetry-equipped cynomolgus monkey. *Front Cardiovasc Med* 2021;**8**:587149.
33. Said MA, Eppinga RN, Lipsic E, Verweij N, van der Harst P. Relationship of arterial stiffness index and pulse pressure with cardiovascular disease and mortality. *J Am Heart Assoc* 2018;**7**(2):e007621.
34. Ziemann SJ, Melenovsky V, Kass DA. Mechanisms, pathophysiology, and therapy of arterial stiffness. *Arterioscler Thromb Vasc Biol* 2005;**25**(5):932–943.
35. Leloup AJ, Van Hove CE, De Moudt S, De Keulenaer GW, Franssen P. Ex vivo aortic stiffness in mice with different eNOS activity. *Am J Physiol Heart Circ Physiol* 2020;**318**(5):H1233–H1244.
36. Bosman M, Krüger DN, Favere K, Wesley CD, Neutel CHG, Van Asbroeck B, Diebels OR, Faes B, Schenk TJ, Martinet W, De Meyer GRY, Van Craenenbroeck EM, Guns PJDF. Doxorubicin impairs smooth muscle cell contraction: novel insights in vascular toxicity. *Int J Mol Sci* 2021;**22**(23):12812.
37. Franssen P, Van Assche T, Guns P-J, Van Hove CE, De Keulenaer GW, Herman AG, Bult H. Endothelial function in aorta segments of apolipoprotein E-deficient mice before development of atherosclerotic lesions. *Pflügers Arch* 2008;**455**(5):811–818.
38. Kausar K, da Cunha V, Fitch R, Mallari C, Rubanyi GM. Role of endogenous nitric oxide in progression of atherosclerosis in apolipoprotein E-deficient mice. *Am J Physiol Heart Circ Physiol* 2000;**278**(5):H1679–H1685.
39. de Mezer M, Rogaliński J, Przewoźny S, Chojnicki M, Niepolski L, Sobieska M, Przystańska A. SERPINA3: stimulator or inhibitor of pathological changes. *Biomedicines* 2023;**11**(1):156.
40. Hurlimann J, van Melle G. Prognostic value of serum proteins synthesized by breast carcinoma cells. *Am J Clin Pathol* 1991;**95**(6):835–843.
41. Han Y, Jia J, Xia X-F, Qin W, Wang S. Combination of plasma biomarkers and clinical data for the detection of sporadic Alzheimer's disease. *Neurosci Lett* 2012;**516**(2):232–236.
42. Boyang C, Yuexing L, Yiping Y, Haiyang Y, Xufei Z, Liancheng G, Yunzhi C. Construction and analysis of heart failure diagnosis model based on random forest and artificial neural network. *Medicine (Baltimore)* 2022;**101**(41):e31097.
43. Delrue L, Vanderheyden M, Beles M, Paolisso P, Di Gioia G, Dierckx R, Verstreken S, Goethals M, Heggermont W, Bartunek J. Circulating SERPINA3 improves prognostic stratification in patients with a de novo or worsened heart failure. *ESC Heart Fail* 2021;**8**(6):4780–4790.
44. Jiang Y, Zhang Y, Zhao C. Integrated gene expression profiling analysis reveals SERPINA3, FCN3, FREM1, MNS1 as candidate biomarkers in heart failure and their correlation with immune in filtration. *J Thorac Dis* 2022;**14**(4):1106–1119.
45. Li B, Lei Z, Wu Y, Li B, Zhai M, Zhong Y, Ju P, Kou W, Shi Y, Zhang X, Peng W. The association and pathogenesis of SERPINA3 in coronary artery disease. *Front Cardiovasc Med* 2021;**8**:756889.
46. Zhao L, Zheng M, Guo Z, Li K, Liu Y, Chen M, Yang X. Circulating Serpina3 levels predict the major adverse cardiac events in patients with myocardial infarction. *Int J Cardiol* 2020;**300**:34–38.
47. Kaur S, Martin-Manso G, Pendrak ML, Garfield SH, Isenberg JS, Roberts DD. Thrombospondin-1 inhibits VEGF receptor-2 signaling by disrupting its association with CD47. *J Biol Chem* 2010;**285**(50):38923–38932.
48. Chistiakov DA, Melnichenko A, Myasoedova V, Grechko A, Orekhov A. Thrombospondins: a role in cardiovascular disease. *Int J Mol Sci* 2017;**18**(7):1540.
49. Xia Y, Dobaczewski M, Gonzalez-Quesada C, Chen W, Biernacka A, Li N, Lee D-W, Frangogiannis NG. Endogenous thrombospondin 1 protects the pressure-overloaded myocardium by modulating fibroblast phenotype and matrix metabolism. *Hypertension* 2011;**58**(5):902–911.
50. Frangogiannis NG, Ren G, Dewald O, Zymek P, Haudek S, Koerting A, Winkelmann K, Michael LH, Lawler J, Entman ML. Critical role of endogenous thrombospondin-1 in preventing expansion of healing myocardial infarcts. *Circulation* 2005;**111**(22):2935–2942.
51. Moura R, Tjwa M, Vandervoort P, Van kerckhoven S, Holvoet P, Hoylaerts MF. Thrombospondin-1 deficiency accelerates atherosclerotic plaque maturation in ApoE^{-/-} mice. *Circ Res* 2008;**103**(10):1181–1189.
52. Munoz-Pacheco P, Ortega-Hernández A, Caro-Vadillo A, Casanueva-Eliceiry S, Aragoncillo P, Egido J, Fernández-Cruz A, Gómez-Garre D. Eplerenone enhances cardioprotective effects of standard heart failure therapy through matricellular proteins in hypertensive heart failure. *J Hypertens* 2013;**31**(11):2309–2318. discussion 2319.
53. van Almen GC, Verhesen W, van Leeuwen REW, van de Vrie M, Eurlings C, Schellings MWM, Swinnen M, Cleutjens JPM, van Zandvoort MAMJ, Heymans S, Schroen B. MicroRNA-18 and microRNA-19 regulate CTGF and TSP-1 expression in age-related heart failure. *Aging Cell* 2011;**10**(5):769–779.
54. Mehri H, Aslanabadi N, Nourazarian A, Shademan B, khaki-khatibi F. Evaluation of the serum levels of mannose binding lectin-2, tenascin-C, and total antioxidant capacity in patients with coronary artery disease. *J Clin Lab Anal* 2021;**35**(10):e23967.
55. Suthahar N, Meijers WC, Silljé HHW, Ho JE, Liu F-T, de Boer RA. Galectin-3 activation and inhibition in heart failure and cardiovascular disease: an update. *Theranostics* 2018;**8**(3):593–609.
56. Fahndrich S, Biertz F, Karch A, Kleibrink B, Koch A, Teschler H, Welte T, Kauczor H-U, Janciauskiene S, Jörres RA, Greulich T, Vogelmeier CF, Bals R. Cardiovascular risk in patients with alpha-1-antitrypsin deficiency. *Respir Res* 2017;**18**(1):171.
57. Meiners B, Shenoy C, Zordoky BN. Clinical and preclinical evidence of sex-related differences in anthracycline-induced cardiotoxicity. *Biol Sex Differ* 2018;**9**(1):38.
58. Norton N, Bruno KA, Di Florio DN, Whelan ER, Hill AR, Morales-Lara AC, Mease AA, Sousou JM, Malavet JA, Dorn LE, Salomon GR, Macomb LP, Khatib S, Anastasiadis ZP, Necela BM, McGuire MM, Giresi PG, Kotha A, Beetler DJ, Weil RM, Landolfo CK, Fairweather D. Trpc6 promotes doxorubicin-induced cardiomyopathy in male mice with pleiotropic differences between males and females. *Front Cardiovasc Med* 2021;**8**:757784.
59. Moulin M, Piquereau J, Mateo P, Fortin D, Rucker-Martin C, Gresseste M, Lefebvre F, Gresikova M, Solgadi A, Veksler V, Garnier A, Ventura-Clapier R. Sexual dimorphism of doxorubicin-mediated cardiotoxicity: potential role of energy metabolism remodeling. *Circ Heart Fail* 2015;**8**(1):98–108.